Reassessing enzyme kinetics: Considering protease-as-substrate interactions in proteolytic networks

Meghan C. Ferrall-Fairbanks[a] ⬤, **Chris A. Kieslich**[a] ⬤, and **Manu O. Platt**[a,1] ⬤

[a]Wallace H. Coulter Department of Biomedical Engineering, Georgia Institute of Technology and Emory University, Atlanta, GA 30332

Enzymes are catalysts in biochemical reactions that, by definition, increase rates of reactions without being altered or destroyed. However, when that enzyme is a protease, a subclass of enzymes that hydrolyze other proteins, and that protease is in a multiprotease system, protease-as-substrate dynamics must be included, challenging assumptions of enzyme inertness, shifting kinetic predictions of that system. Protease-on-protease inactivating hydrolysis can alter predicted protease concentrations used to determine pharmaceutical dosing strategies. Cysteine cathepsins are proteases capable of cathepsin cannibalism, where one cathepsin hydrolyzes another with substrate present, and misunderstanding of these dynamics may cause miscalculations of multiple proteases working in one proteolytic network of interactions occurring in a defined compartment. Once rates for individual protease-on-protease binding and catalysis are determined, proteolytic network dynamics can be explored using computational models of cooperative/competitive degradation by multiple proteases in one system, while simultaneously incorporating substrate cleavage. During parameter optimization, it was revealed that additional distraction reactions, where inactivated proteases become competitive inhibitors to remaining, active proteases, occurred, introducing another network reaction node. Taken together, improved predictions of substrate degradation in a multiple protease network were achieved after including reaction terms of autodigestion, inactivation, cannibalism, and distraction, altering kinetic considerations from other enzymatic systems, since enzyme can be lost to proteolytic degradation. We compiled and encoded these dynamics into an online platform (https://plattlab.shinyapps.io/catKLS/) for individual users to test hypotheses of specific perturbations to multiple cathepsins, substrates, and inhibitors, and predict shifts in proteolytic network reactions and system dynamics.

computational modeling | cysteine cathepsins | extracellular matrix | proteolysis

The implicit assumption of protease inertness, where proteases only hydrolyze substrate(s) and only negligible degradative interactions occur between proteases in solution, dominates the protease literature. However, this assumption must be reconsidered when considering proteases working as a part of a system or a proteolytic network with multiple classes of proteases, substrates, and inhibitors (1). Important work has been done on protease families that contain members that hydrolyze each other to activate zymogens, or inactive forms, converting the inactive protease to the mature, active protease form, but less so on destructive hydrolysis that removes a protease from the pool able to actively proteolyze substrate. There are also families of promiscuous proteases such as the cysteine cathepsins, a potent family of proteases first identified in lysosomes where they serve important roles in protein turnover, but that have since been implicated in a number of other intracellular and extracellular compartments and are up-regulated in a number of tissue-destructive diseases (2–8). Cysteine cathepsins are synthesized as procathepsins, with a propeptide occluding the active site, which must be cleaved to have mature, active enzyme (2, 3). Propeptide cleavage has been reported to occur through autocatalysis, as well as through cleavage by another protease (5, 9–11). It is difficult to

analyze how these proteases interact cooperatively or antagonistically, and researchers have only recently started to investigate these types of interactions (1, 12–14).

Of interest to this work are cathepsins K, L, and S (catK, catL, and catS), which share 60% sequence identity and redundancy in target substrate proteins with different catalytic activities toward different matrix substrates (2, 5, 15). These cathepsins are involved in a number of diseases and have been targets of pharmaceutical companies to design inhibitors. However, of the 16 inhibitors that have progressed to phase II and III clinical trials, none have made it to the medicine cabinet (16–18).

Previously, we have shown that, when catK and catS were coincubated together, the total amount of substrate degradation from the equimolar amounts of cathepsins was less than the sum of the individual cathepsins' proteolytic activity (12). The catS preferentially binding and degrading catK over the substrate was introduced and could accurately capture the amount of substrate degradation (12), even such that mutating the sites susceptible to cannibalistic cleavage reduced the amount of catK cleaved by catS, effectively creating cannibalism resistant catK mutants (14). In another study, catK and L interactions were important in tendon extracellular matrix (ECM) degradation in vivo (19), and the sequence of cathepsin addition to the system, whether secreted by the cells in vivo, or with addition of recombinant

---

Significance

Proteases are enzymes that hydrolyze other proteins, including other proteases, which challenges assumptions of enzyme inertness in chemical reactions, and alters predicted protease–substrate concentrations using established mass action frameworks. Cysteine cathepsins are powerful proteases involved in numerous diseases by cleaving substrates, but they also hydrolyze each other, requiring inclusion of as yet undefined, protease-as-substrate dynamics. Here, we used experimental and computational models to improve predictions of the concentrations of multiple species and intermediates generated during substrate degradation in multiprotease systems by including protease-on-protease reactions of autodigestion, inactivation, cannibalism, and distraction in proteolytic networks. This was made available online for others to test perturbations and predict shifts in proteolytic network reactions and system dynamics (https://plattlab.shinyapps.io/catKLS/).

enzyme addition in vitro, contributed to total substrate degradation due to cannibalistic interactions between catK and L (20).

To expand upon our knowledge of the cathepsin proteolytic network and its impact on substrate degradation and enzyme kinetic models, here we developed a mechanistic model consisting of a system of ordinary differential equations characterizing the catK, L, and S proteolytic network with elastin and gelatin substrates. We use a systematic approach to 1) characterize the kinetics of individual cathepsins on substrates elastin or gelatin in this system; 2) incorporate cathepsin-on-cathepsin binding and catalytic interaction rates for each pair of catK, L, and S; and 3) integrate all three cathepsin interaction and substrate degradation activities. With this cathepsin proteolytic network model, we predicted substrate degradation a priori of all three cathepsins at once and simulated the effects of changes to this proteolytic network for additional substrates and for the genetic disease pycnodysostosis, caused by mutations in the catK gene, to demonstrate the utility and importance of considering protease-as-substrate kinetics when deriving systems of protease degradation and inhibition in complex biological systems.

Results

Combinations of Cathepsins Cleaving Substrates Yield Nonintuitive and Substrate-Dependent Amounts of Product Formed.
Incubating catK, L, and S systematically in one-, two-, and three-cathepsin combinations led to nonintuitive results for substrate proteolysis that were substrate-dependent. Five picomoles of each cathepsin were incubated with fluorogenic elastin or gelatin (Fig. 1 *A* and *B*) (21). If the proteases were inert to each other, then coincubating catK, L, and S together with substrate would be expected to cleave the highest amount of substrate, generating the highest quantity of product, since that system would contain three times the molar concentration of proteases compared to that of a single cathepsin incubated with substrate. On gelatin, the three-cathepsin combination generated the highest amount of product (Fig. 1*B*), but, on elastin, the three-cathepsin combination generated product amounts that clustered with one- and two-cathepsin combinations (Fig. 1*A*). To interpret: Equivalent molar amounts of catK and S in the catK+S combination were in the combination of catK+S+L; for elastin, the presence of catL did not lead to increased elastin degradation, but catL did cause significant elevation in total gelatin degraded in the system—more than its solo contribution to gelatin degradation.

Stepwise Determination of Multimember Proteolytic Network Interactions.
Mass action kinetics was the basis for constructing a mathematical model of proteolysis. A system of ordinary differential equations implemented mass action kinetics to mechanistically describe the cathepsin−substrate and cathepsin−cathepsin interactions (22). The canonical form of mass action kinetics (23–25) for dependent variables, X_i, are described by

$$\frac{dX_i}{dt} = \sum_{k=1}^{T_i} \left(\pm \gamma_{ik} \prod_{j=1}^{n+m} X_j \right),$$ [1]

where n is the number of dependent variables, m is the number of independent variables, T_i is the number of terms in the ith equation, and γ_{ik} are reaction rate constants (26). To develop a mechanistic model of the cathepsin proteolytic network, parameters were systematically estimated for a traditional mass action enzyme kinetics system with one enzyme and one substrate (Fig. 1*C*). Kinetic rates were estimated using a surrogate-based optimization algorithm and parameter bounds based on known physical and biological limits (*Methods*) with substrate in high excess, and were then compared to the individual contributions of either catK, L, or S to degrading elastin and gelatin (Fig. 1 *D* and *E*). Across all cathepsins and all substrates, substrate hydrolysis reactions

alone could not accurately predict product formation by an individual cathepsin whether it was catK, L, or S over this time frame of 120 min, and is represented as the straight line (Fig. 1 *F*–*K*).

Underlying assumptions that the proteases are catalysts that do not get used or modified in the mass action kinetics overpredicted the product formation by cathepsins and required some terms that reduced the amount of active protease, since the substrate concentration was not limiting. When a protease can also be the substrate, as well as the enzyme in the system, there is a loss of enzyme over time that must be considered. To accommodate this, the model was modified to include terms of autodigestion, defined as one active cathepsin binding to another active cathepsin of the same type and hydrolyzing it, resulting in one free, active cathepsin and one degraded cathepsin (Fig. 1*C*). This mechanism has been previously shown to occur for cathepsin family members (9–11). Another mechanism by which active cathepsins are lost to the system is inactivation. Cysteine cathepsins prefer an acidic, reducing environment to maintain their proteolytic activity and can be inactivated under neutral pH or oxidizing environments. To include cathepsin inactivation, we incorporated a rate for converting active to inactive protease. The inactivation rate was fit as a linear process with one kinetic rate, k_{inact}. The models including autodigestion and inactivation terms greatly improved the prediction of the overall substrate degradation, compared to the simpler, inert model (Fig. 1 *F*–*K*). During parameter estimation, the autodigestion and inactivation rates were held constant across the two substrates and assumed to be substrate-independent, since they are inherent properties of the enzymes. For catK, total cathepsin equaled active cathepsin, because catK had the highest rate of autodigestion. The catS and L, on the other hand, were more susceptible to inactivation, as indicated by there being a difference in the total protease levels and the active amounts. These results support previous data published by us that catK, when incubated alone, does not have immunodetectable protein, but catS and L do (12, 20).

Once individual cathepsin dynamic parameters were fit, models of proteolytic pairs were constructed, inclusive of autodigestion and inactivation reaction terms. Paired proteolytic interactions were modified to include two more terms, cannibalism and distraction, because assumptions of inert reactions between the two proteases implied additive substrate degradation (Fig. 2*A*), but, from the observed experimental results, this overpredicted the actual, measured substrate degraded (Fig. 2 *B*–*D*). Cathepsin cannibalism was defined as cathepsin-on-cathepsin binding and hydrolysis, with the hypothesis that active protease-on-active-protease interactions reduced the amount of active enzyme available to bind and degrade substrate. Distraction was a term included where degraded or inactive enzyme could still be bound by active enzyme, distracting it from degrading the putative, target substrate. Cannibalism was used as a descriptor for active enzyme binding and hydrolyzing active enzyme; distraction was the term for active enzyme binding and hydrolyzing inactive/degraded enzyme. In this work, we assumed that the kinetic rates associated with binding and degrading of the active and inactive forms were identical.

Incorporating cathepsin cannibalism and distraction interactions greatly reduced the normalized error compared to the case predicted by inert proteases and superposition on elastin (Fig. 2 *B*–*D*) and gelatin (Fig. 2 *E*–*G*). The amount of active catK was greatly reduced by coincubation with catS (Fig. 2*H*). Notably, in the paired proteolytic network model of catK and L, the calculated amount of active catL was rapidly reduced to almost zero by 60 min when, in the absence of cannibalism, catL concentration does not go below 10 nM after 120 min (Fig. 2*I*), suggesting that catK cleavage of catL may serve to reduce amounts of catL, as catS appears to do to catK. Finally, for the catS and catL pair, there were increases of less than 1 nM in amount of active catS for each time point, and little change in the amount
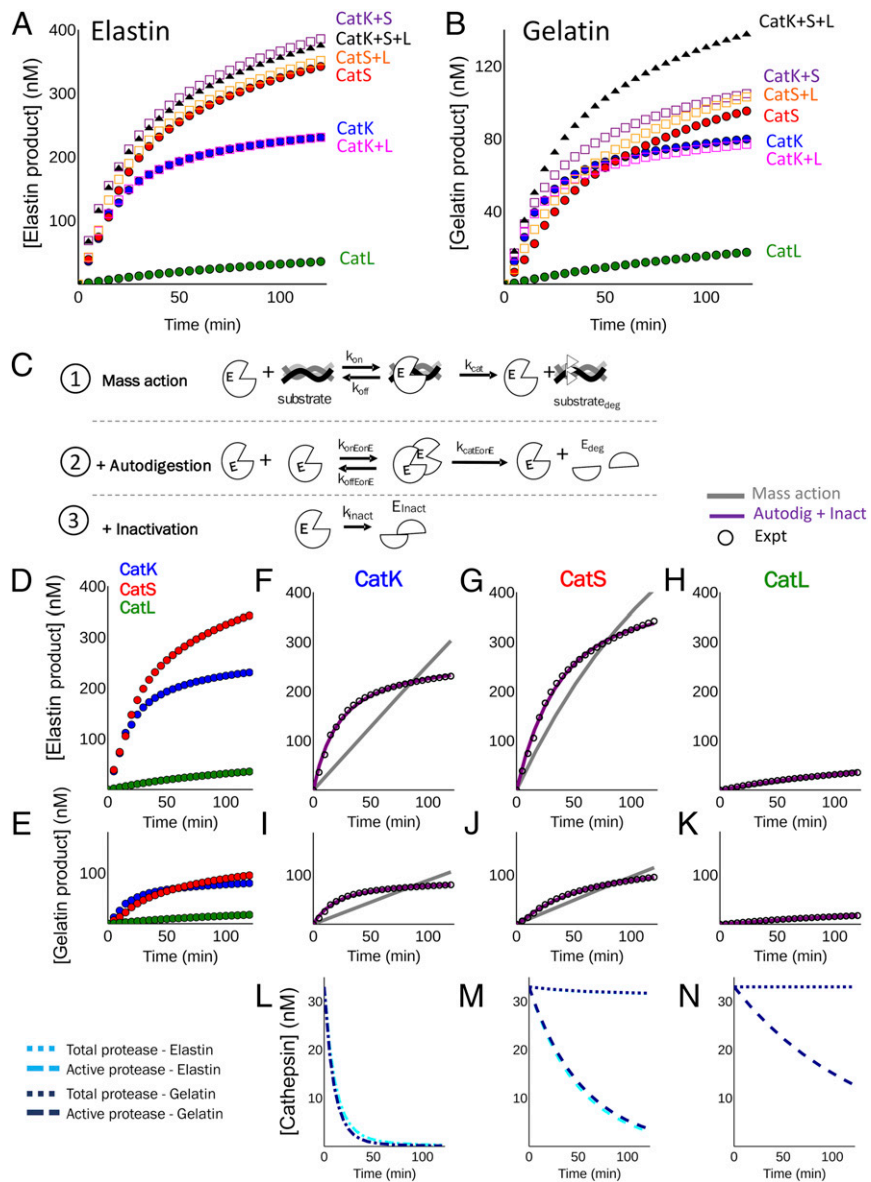
Fig. 1. Comparison of the degradation of elastin and gelatin by catK, catL, and catS. The catK, catL, catS, and catV working in concert do not degrade the most elastin and gelatin. Kinetic study fluorescence data of cathepsin individuals, pairs, and triplet groups incubated on fluorogenic elastin or gelatin substrates indicate degraded product generated differs based on protease combination. (*A*) Time course data for degradation of elastin by combinations of one, two, or three catK, catL, and catS. (*B*) Time course data for degradation of gelatin by combinations of one, two, or three catK, catL, and catS. (*C*) Schematics of three model structures evaluated to describe degradation of substrate by cathepsin K, S, or L: (*1*) mechanism of mass action reaction to describe substrate degradation, (*2*) autodigestion terms were added to extend the mass action model, and (*3*) inactivation terms were added. (*D* and *E*) Comparisons of experimental data (Expt, black points) for (*D*) degraded elastin or (*E*) degraded gelatin to predictions for the three models over 120 min. (*F–H*) Calculated elastin product generated by (*F*) catK, (*G*) catS, and (*H*) catL are shown, and (*I–K*), respectively, for gelatin product. (*L–N*) Comparisons of the active and total cathepsin (*L*) K, (*M*) S, and (*N*) L concentrations were also pulled from the model and presented. Of those, catK was lost through autodigestion (Autodig), thus the difference between total and active, but catS and L were lost more through inactivation (Inact).

of active catL (Fig. 2*J*). The full list of equations is provided in *SI Appendix*, Table S1 containing the parameters for the individual cathepsin reactions, *SI Appendix*, Table S2 containing the paired cathepsin reactions, and the corresponding parameter estimation errors (normalized error) reported in *SI Appendix*, Table S3.

Individual and paired kinetics predict triple protease network outcomes, a priori. Paired protease parameters were used to create a triplet proteolytic network for catK, L, and S, coincubated, all working in one system. The prediction closely fit the experimental data from the triplet proteolytic network on elastin (Fig. 3*A*) and slightly underpredicted the cumulative network proteolysis for gelatin (Fig. 3*A*), a priori. The catalytic efficiencies highlighted

that catL was the least efficient and catK was the most efficient (Fig. 3*B*). Likewise, for the protease-on-protease interactions, the catK on K, catK on L, catL on K, and catS on K were the most efficient of the cannibalistic interactions (Fig. 3*C*).

After validating the three-cathepsin proteolytic network model, incorporating cannibalism, distraction, inactivation, and autodigestion against the three-cathepsin experimental data, the next goal was to perturb the interactions to determine net effects on putative substrate degradation under different situations. The catK was the focus, since it had the highest catalytic efficiency and participates in autodigestion and cannibalistic interactions. In silico experiments were conducted to quantify how
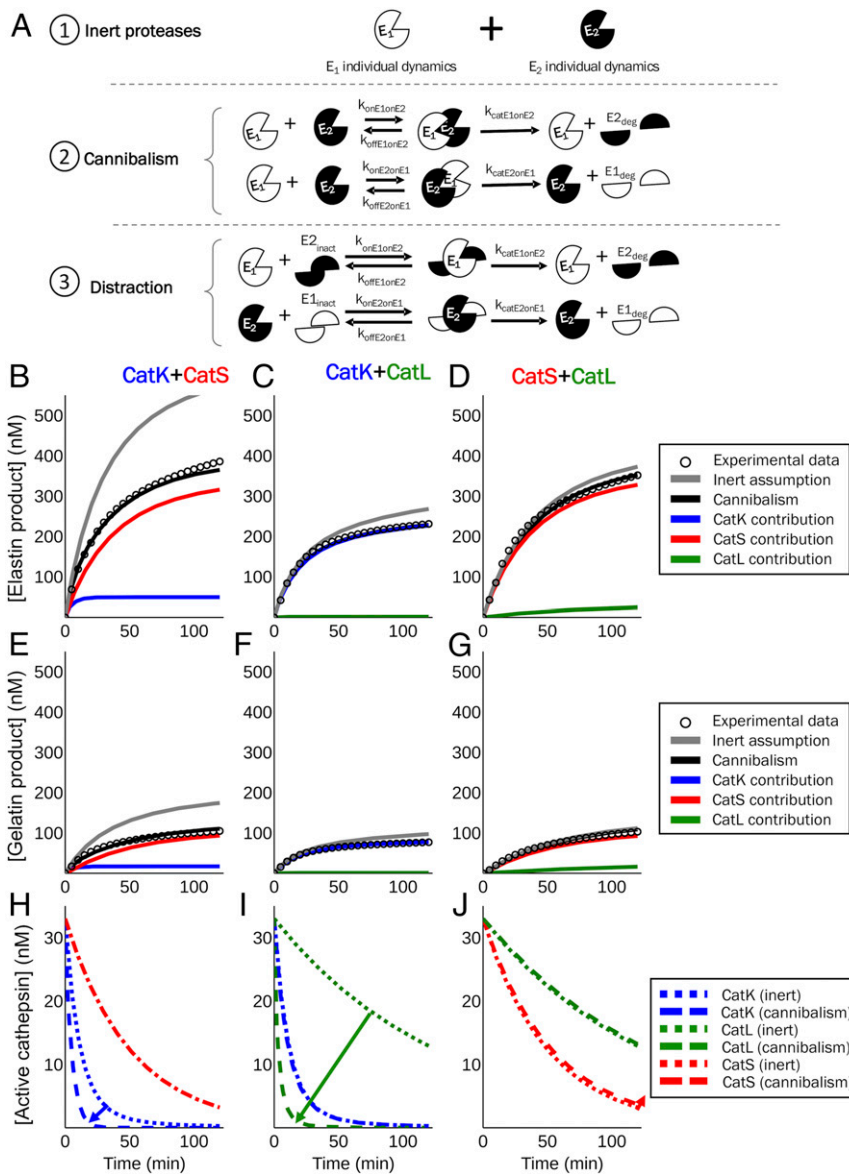
Fig. 2. Cathepsin–cathepsin proteolytic interactions were necessary to accurately describe paired cathepsin substrate degradation and account for loss of active enzyme. (A) Schematics of the changes to the model structures to include protease interactive terms, to modify the interactions from 1) assuming the proteases were inert to each other, only binding to and hydrolyzing substrate which would cause additive product generation; 2) cannibalism terms incorporating active cathepsin binding to and degrading other active cathepsins; and 3) distraction terms with active cathepsins binding to inactive cathepsins and degrading them. (B–G) Comparisons of experimental data (black points) for (B–D) degraded elastin or (E–G) degraded gelatin over 120 min to the model predictions under the inert scenario (gray line) and for a scenario inclusive of the cannibalism and distraction interactions (black line). Models of the paired cathepsin interactions after incubation are shown: (B) catK and catS, (C) catK and catL, (D) catS and catL for elastin and (E–G) on gelatin. The contributions of each individual cathepsin are graphed as well, with catK in blue, catS in red, and catL in green. Inert model (gray line) over predicted substrate degradation for all pairs, with the catK+catS pair being the most significantly over predicted due to the strong cannibalism of catK by catS. Dotted lines represent the inert condition, and dashed lines represent the cannibalism condition. When a dot-dash line is visible, this means that the two conditions directly overlap, and comparing inert and cannibalism had no difference. (H–J) Comparisons of active cathepsin concentrations show that catK was being cannibalized by catS, and catL was being cannibalized by catK, while distraction interactions between cathepsins S and L lead to preservation of active enzyme. Arrows added for emphasis.

modulating interactions between catK and catS or L would change total elastin degradation. To do so, autodigestion and cannibalism catalytic rates were reduced by orders of magnitude to determine how each of these reactions that could cause loss of enzyme might affect total substrate degradation (Fig. 3 D–F). Changes in active cathepsin concentrations were also monitored (Fig. 3 G–I). Reducing catK autodigestion catalytic rate to 1/1,000th did not appreciably increase elastin degradation in the three-cathepsin proteolytic network (Fig. 3D). There was much

more catK present, however, with the reduced catK autodigestion rate and even a small increase in catL at first, resulting in less catL by 120 min, due to catK cannibalism of catL (Fig. 3G). The catS concentrations appeared to play a critical role in protecting elastin from excess degradation by catK; reducing the catS on catK cannibalistic rate of catalysis by to 1/10th greatly increased the predicted amount of elastin degradation, by almost 30% (Fig. 3E). Calculations of protease concentrations provided insight into these outcomes; increased amount of active catK was
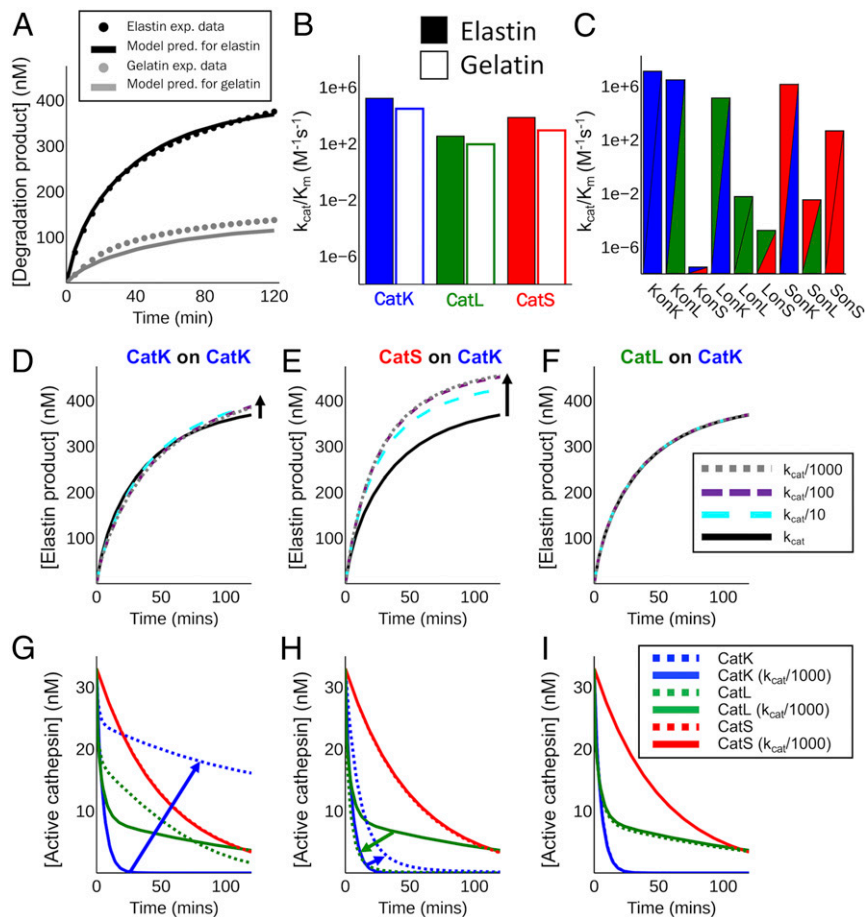
Fig. 3. Combination of individual and paired cathepsin models predicts, a priori, the outcomes of triple cathepsin proteolytic network interactions. (*A*) Parameters from individual and paired models were used to test their predictability of triple cathepsin network outputs of elastin (black) and gelatin (gray) degradation, shown as solid lines. Model outputs were compared to experimental (exp.) data for 120 min and indicate low error between predicted (pred.) and observed responses. (*B*) Catalytic efficiencies (k_{cat}/K_m) for catK, L, and S degradation of elastin (solid) and gelatin (open) calculated from model parameters. (*C*) Cannibalistic and autodigestion catalytic efficiencies were calculated, highlighting important contributions of catK on K (KonK), catL on L (LonL), and catS on S (SonS) autodigestion and cannibalism relationships of catK on L (KonL), catL on K (LonK), catK on S (KonS), catS on K (SonK), catL on S (LonS), and catS on L (SonL). (*D*) The catK autodigestion rates were reduced by 10-, 100-, and 1,000-fold, but there was no appreciable increase in elastin degradation. (*E*) The catS on catK cannibalism catalytic rate was similarly modified; reducing this to 1/10th greatly increased predicted elastin degradation, by almost 30%, with further increases as this rate was reduced to 1/1,000th of fit parameter. (*F*) Reducing catL on catK cannibalistic rate had no effect. (*G*) Reduced catK autodigestion rate by 1,000-fold increased amount of active catK (blue arrow) with a concomitant reduction in catL (green solid line to green dotted line) due to catK cannibalism of catL. (*H*) Increased active catK occurred when catS on catK cannibalism was reduced by 1,000, but less than autodigestion effect, and, again, associated with reductions in catL. (*I*) Reducing catL's cannibalistic rate on catK had no effect on protease concentrations.

present when catS's cannibalism was reduced (Fig. 3*H*), allowing more catK to bind and hydrolyze elastin. Reducing catL's cannibalistic rate on catK did not lead to a change in elastin degradation (Fig. 3*F*) or protease concentrations (Fig. 3*I*), even at 1,000-fold decreased catalytic rates, but this reflects the poor catalytic efficiency of catL on catK.

Impact of Distraction Interactions on Substrate Degradation. Distraction effect of inactive proteases was further explored to determine consequences of these interactions in the triple cathepsin proteolytic network. To test the hypothesis that distraction interactions protect substrate from degradation, we simulated increasing concentrations of inactive cathepsins to calculate the effects of distracting active enzyme on total substrate degradation (Fig. 4 *A*–*C*) and active enzyme levels in the system (Fig. 4 *D*–*F*). Increased amounts of inactive catK provided the greatest distraction for both catS and L, with a huge reduction in predicted degraded elastin (Fig. 4*A*), and similarly large increases in active catS and L in the presence of 1,000-fold inactive catK (Fig. 4*D*). Inactive catL had a similar effect on catS and K (Fig. 4*B*),

reducing elastin degradation by distracting the active protease that bound catL instead of substrate. Increased amounts of inactive catS in the presence of catK and L did not change the calculated amount of either substrate degradation (Fig. 4*C*) or active enzyme (Fig. 4*F*).

Cases of Pycnodysostosis: Genetic Mutations for Loss of Active catK. Since protease-on-protease and distraction interactions were demonstrated to affect amounts of active proteases in a multi-member proteolytic network, pathological examples were implemented in this triplet proteolytic network model. In healthy individuals, catK is highly expressed in osteoclasts and critical in degradation of type I collagen during bone resorption and remodeling processes (27). Pycnodysostosis is a very rare disease caused by mutated catK with a prevalence of 1 to 1.7 individuals per million. Due to loss of active catK, these patients have increased bone density, skeletal dysplasia, skull deformities, and increased bone fragility and fractures (28, 29). While individuals with pycnodysostosis have normal numbers and morphology of osteoclasts, upon ultrastructural examination, they have abnormal
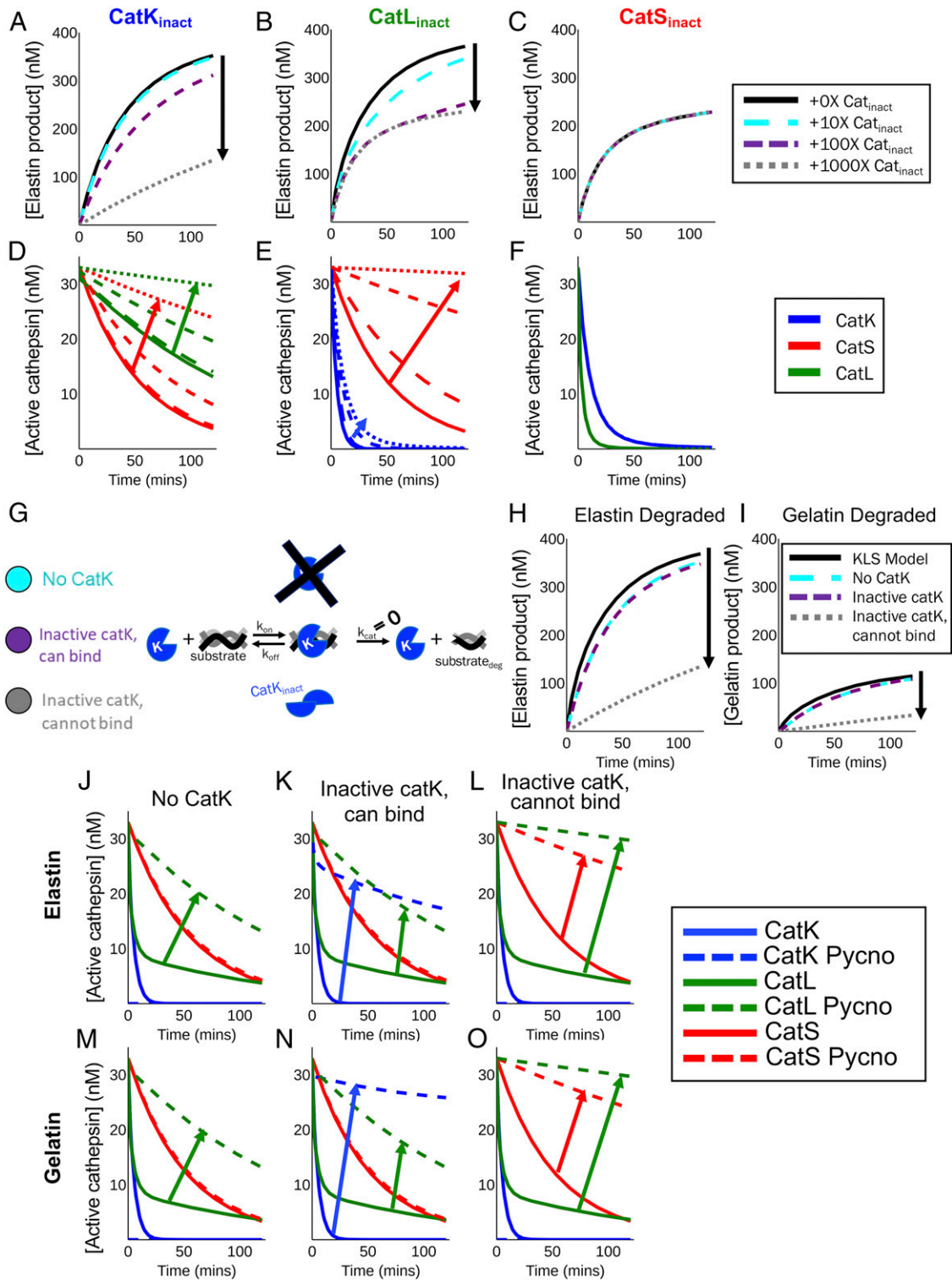
Fig. 4. Distraction interactions reduce substrate degradation, while extending amounts of active cathepsins: relevance for genetic disease pycnodysostosis. Simulations were performed for each cathepsin pair, where increasing amounts of the third cathepsin in its inactive form were introduced to test consequences of distraction interactions. (*A*) The catS and catL with inactive catK; (*B*) catK and catS with inactive catL; and (*C*) catK and catL with inactive catS. Degraded elastin, in the presence of 0×, 10×, 100×, and 1,000× concentrations of distracting cathepsin, is shown. (*D*–*F*) Respective corresponding predictions of active cathepsin concentrations. Distraction induced increased active proteases, yet still caused reduced elastin degradation. Arrows added for emphasis. (*G*) Schematic representation of pycnodysostosis (Pycno) models. "No catK" case represents mutation causing no catK protein to be produced. "Inactive catK, can bind" represents mutated catK able to bind substrate but not catalytically active. "Inactive catK, cannot bind" represents mutated catK as a fully distracting species, no binding and no catalysis, modeled at 1,000-fold concentration. (*H* and *I*) Using pycnodysostosis models, amounts of degraded elastin and gelatin were predicted, with largest reduction predicted for fully distracting scenario where catK was inactive and could not bind substrate. (*J*–*O*) Predictions of active cathepsin concentrations are shown for three pycnodysostosis models in presence of (*J*–*L*) elastin and (*M*–*O*) gelatin. All three scenarios resulted in increased active catL, while the full distraction scenario also predicted significant increases in active catS as well. Arrows added for emphasis.

cytoplasmic vacuoles with collagen fibrils and other bone matrix proteins that would otherwise have been degraded by non-mutated, catalytically functioning catK (28–30). In individuals with pycnodysostosis, the catK gene has a mutation that can 1) cause no detectable catK in cells, 2) cause catK protein to be synthesized, and binds to substrate, but is not catalytically active, or 3) cause catK protein to be synthesized that is inactive, and does not bind to substrate (28–30). The latter two cases are both examples of potential distraction scenarios where inactive catK can still be targeted by its cannibalistic family members, distracting them from substrate in the system.

The cathepsin proteolytic network of catK, L, and S in an individual with pycnodysostosis was modeled in silico to reflect conditions 1, 2, and 3 above (Fig. 4G) to determine net effects on elastin and gelatin degradation (Fig. 4 H and I) and consequences for levels of inactive catK, and active catL and S. If no catK were present, one would expect similar substrate degradation as in the catL/S paired network. However, the model predicted a large increase in active catL and miniscule increase in the amount of active catS (Fig. 4 J and M) compared to the situation with all three functioning cathepsins present, with no difference between substrates. To simulate the pycnodysostosis scenario of catK being present, but inactive and capable of binding substrate, but not cleaving it, all catK catalytic rates were set to zero. Comparable substrate degradation was predicted (Fig. 4 H and I), but active cathepsin dynamics were vastly different; with no autodigestion, catK was still present by 120 min, as was the predicted amount of active catL, since it was no longer susceptible to catK cannibalistic hydrolysis (Fig. 4 K and N).

For the scenario defined as inactive catK that could neither bind nor degrade substrate, pycnodysostosis was modeled such that only inactive catK was present, and all catK k_{on} binding and catalytic rates were set to zero. Inactive catK concentrations were initially set as 1,000-fold higher to model accumulated inactive catK at time zero. This resulted in the inactive catK distracting catS and L from binding to elastin and gelatin substrates, resulting in over 50% reduction in predicted substrate degradation (Fig. 4 H and I) compared to the nonpycnodysostosis, three-cathepsin model, coincident with almost 200% increases in the predicted amount of active catS and L in the system (Fig. 4 L and O). These protease levels were higher, as they were being distracted from binding to and degrading target substrate, binding instead to inactive catK that was not being removed from the system by autodigestion.

Interactive, Online Interface of Three-Cathepsin Dynamic Proteolytic Network. The proposed proteolytic network model could have potentially broader utility for the study of proteases and general protein turnover, and the full model schematic containing autodigestion, inactivation, cannibalism, and distraction is presented in Fig. 5A. To make these developed models broadly accessible, we developed an interactive online interface using R Shiny (31) that allows model inputs to be manipulated by users, with updated predictions provided in real time. Shiny is an open source package for the R statistical language that streamlines the process of making interactive R code available online (31–33). We have used the R Shiny framework to develop an interactive interface for a model that predicts the amount of substrate degraded with multiple cathepsins working on either gelatin or elastin based on data and parameters derived from this report, now available at https://plattlab.shinyapps.io/catKLS/.

This cathepsin-specific interface is preconfigured with parameters determined for the cathepsin K, L, and S proteolytic network containing autodigestion, inactivation, cannibalism, and distraction interactions and allows users to manipulate system inputs, such as the initial cathepsin or substrate concentrations, and also contains inhibitor inputs as well, since we have a goal of assisting cathepsin pharmacological inhibitor development. Outputs are predictions

of substrate degradation, amounts of active and inactive proteases (Fig. 5B), and various intermediates, including concentrations of protease complexes, and degraded cathepsins (Fig. 5B).

To provide users with further options for exploring model predictions, the interface utilizes the R wrapper for plotly (33) when plotting the model predictions, which provides dynamic plots that include features such as zoom. The proposed interface also includes automated report generation, where R Markdown (34) is used to generate PDF documents containing the model inputs and all of the plots visualizing the predictions. The interface allows for export of simulation data in the form of .CSV files that users can download for more specific analysis offline or more independent plot generation.

Reduced Model of catK, L, and S Proteolytic Network. Putative autodigestion, inactivation, cannibalism, and distraction interaction terms were parameterized and included for all possible interactions in the three-cathepsin proteolytic network and included in the Shiny app online model. This provides a platform for others who are modeling kinetics and outcomes from proteolytic reactions to use. However, reduced models can be made after identifying the most significant interactions within the specific proteolytic network, which also reduces computational time. For the cathepsin K, L, and S proteolytic network model, we used the computed catalytic efficiencies for autodigestion and cannibalism reactions (Fig. 3C) to identify that catK on K, catK on L, catL on K, and catS on K reactions were the most significant. Additionally, inactivation rate of catK ($7.494e{-}10$ s^{-1}) was insignificant compared to inactivation rates of catS ($1.906e{-}2$ s^{-1}) and catL ($7.810e{-}3$ s^{-1}) under these conditions, so it could be excluded.

By assuming that low contributing reactions were not significant to the outcome and removing them from the system of equations, the reduced model contained 32 parameters and 15 dependent variables, substantially reduced from the full model with 48 parameters and 29 dependent variables. The reduced model provided comparable a priori predictions for substrate degradation by all three proteases in combination (Fig. 6A) compared to experimental data and the full triplet model (Fig. 3A). The reduced model also recapitulated contributions of catK, L, and S to elastin and gelatin degradation (Fig. 6B), as well as relative contributions of autodigestion and cannibalism interactions in terms of catalytic efficiency (Fig. 6C). In this reduced version, a few reactions to note are as follows: 1) Autodigestion and cannibalism by catS dominate removal of catK from the system, 2) inactivation is the dominant mechanism to remove catS, and 3) catL is susceptible to inactivation and to cannibalism by catK for its removal from the system. These reactions are shown in the reduced model schematic (Fig. 6D).

Discussion

This study demonstrates that protease-on-protease interactions can occur that alter expected outcomes from traditionally considered enzyme kinetics. The example case here demonstrated that cathepsin–cathepsin interactions of autodigestion, inactivation, distraction, and cannibalism occur between catK, catL, and catS, which reduced the amount of active enzyme in the system and thereby reduced the amount of substrate degradation from what could have occurred if the proteases were inert to acting on each other. Proteases are different from other enzymes in that they can hydrolyze each other to remove each other from the system, particularly in the case of the cysteine cathepsins that can play roles in nonspecific protein degradation in lysosomes, but are also upregulated and even secreted in disease states (35). Using a systematic approach, a cathepsin proteolytic network model of catK, catL, and catS degrading elastin or gelatin substrates was constructed and had the rates incorporated into a user-friendly, online interface of the computational model for broader distribution and use. Inactivation of proteases and autodigestion by proteases were
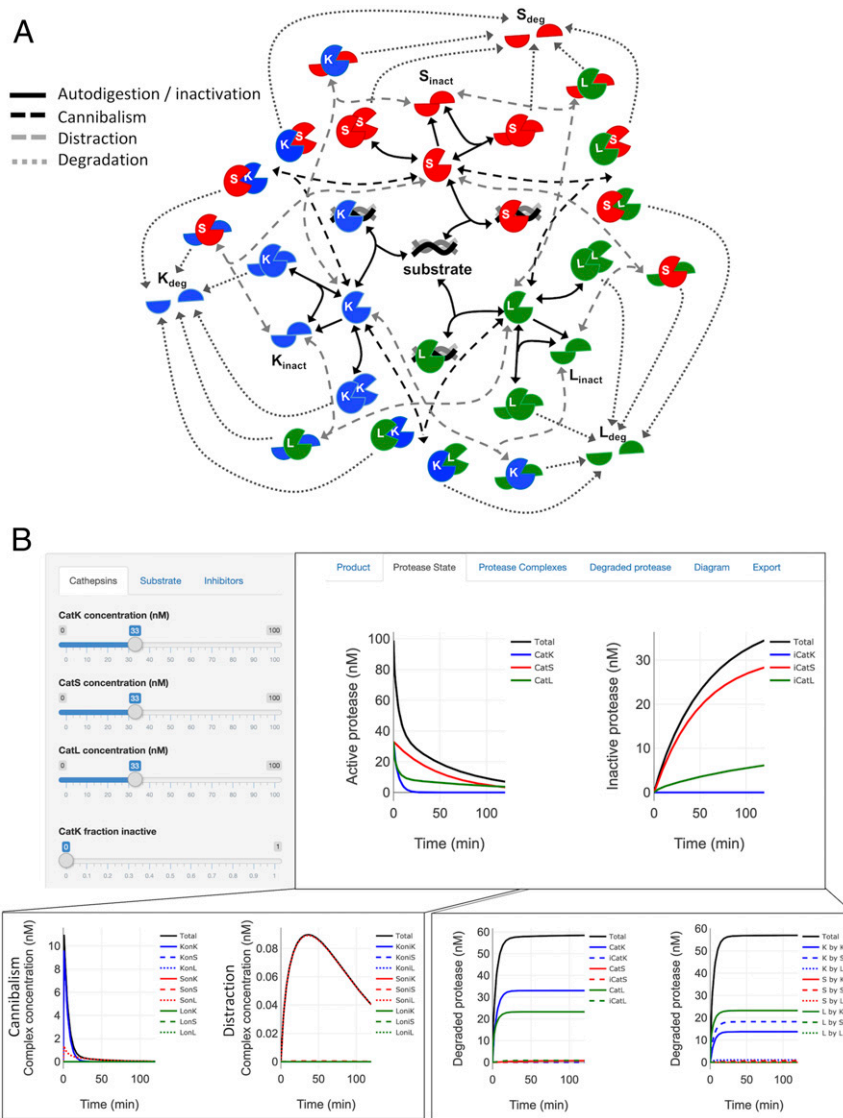
Fig. 5. Interactive online interface of three-cathepsin dynamic proteolytic network. (*A*) Full triple cathepsin proteolytic network model schematic containing autodigestion, inactivation, cannibalism, and distraction interactions. (*B*) Screen shot of the online application available at https://plattlab.shinyapps.io/catKLS/. The online application provides an intuitive interface that allows the user to alter enzyme and substrate concentrations, as well as other system variables and parameters. Additional graphs that can be generated and are shown in the screenshot are amounts of active and inactive proteases, and various intermediates, including concentrations of protease complexes, and degraded cathepsins.

both necessary reactions to consider and include to fit experimental data in single-protease systems. Cathepsin cannibalism was also occurring between the pairs of proteases as contributors to additional loss of active enzyme from the system. There was also cleavage of cathepsins that became inactivated by active proteases, that distracted active proteases from substrate degradation, adding another reaction term that could have significant impact on total substrate degraded under certain conditions. Kinetic rates from the individual and paired cathepsin interactions were sufficient to predict substrate degradation by all three cathepsins when coincubated. To present the consequences of cannibalism and distraction on physiological systems, the case of pycnodysostosis was simulated, by which there are three ways that genetic mutations to catK gene impact the amount of substrate degradation and the amounts of active cathepsins in the system. Large amounts of inactive catK in the system have the potential to be a distraction to other proteases, distracting them from degrading substrate, more so than if the mutation led to no catK being produced at all. Taken

together, these results indicate that cathepsin degradation of other active cathepsins or being distracted by binding to and hydrolyzing inactive cathepsins reduces degradation of target substrate from predictions that assume proteases were inert to each other.

This work demonstrates that complex cathepsin−cathepsin interactions are modulating the concentrations of cathepsins catalytically active toward substrates in a system. The cathepsin−substrate binding and catalytic rates determine to what extent these cathepsin−cathepsin interactions modulate the amount of active enzyme in the system. Autodigestion and inactivation rates were cathepsin-specific, and a protease working on itself is not immune to altering the rest of the network, since it could be a substrate for other proteases. Using our Protease-Ase Cleavages from MEROPS Analyzed Specificities (PACMANS) analysis tool (14) to identify potential cleavage sites on catK, catL, and catS by each other, we predict top scored putative cleavage sites for catK at L253 and V171, for catL at L156, E176, V239, and S326, and for catS only at L159. The catK sites were mutated to
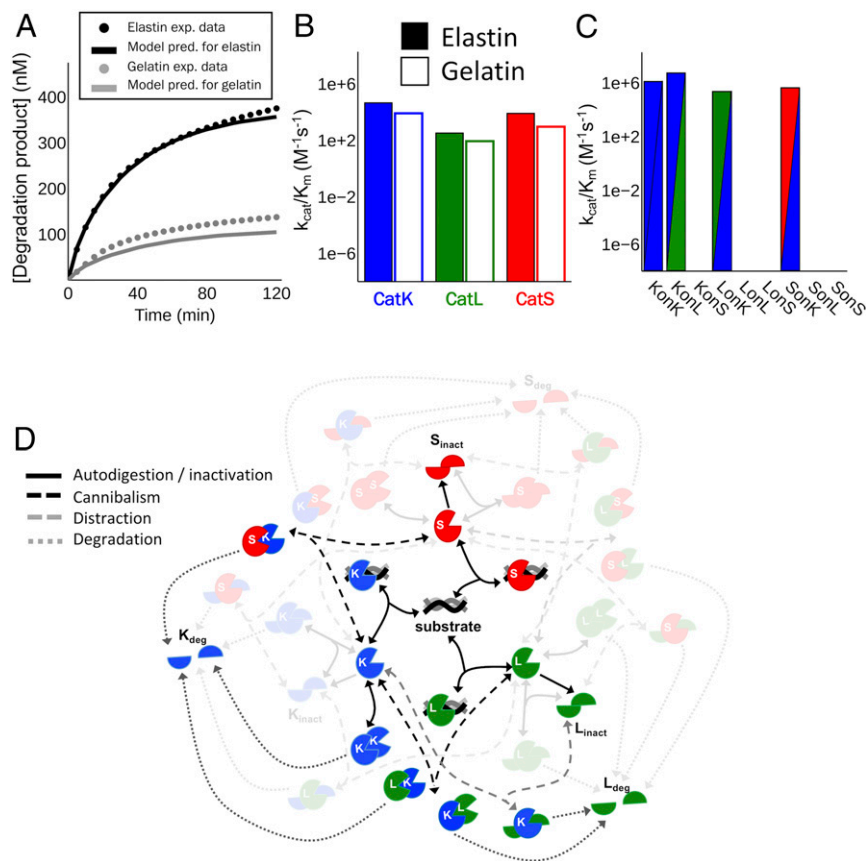
Fig. 6. Reduced model of cathepsin K, L, and S proteolytic network. A reduced model was parameterized by identifying processes with largest contribution in the full model. (*A*) The reduced model predicts substrate degradation for the catK, L, and S triple cathepsin proteolytic network with accuracy comparable to the full model. The solid points indicate experimental data for degraded elastin (black) or degraded gelatin (gray) over 120 min, while the solid lines indicate the corresponding model predictions. (*B*) Reduced model predicted similar catalytic efficiencies (k_{cat}/K_m) for catK, L, and S on elastin (solid) and gelatin (open). (*C*) Similar cannibalistic and autodigestion catalytic efficiencies were also predicted compared to the full model. (*D*) Schematic of the reduced model for catK, L, and S that includes the most contributing interactions for this proteolytic network. Even the reduced model includes autodigestion, inactivation, cannibalism, and distraction interactions, but differs for each of the cathepsins included.

generate catK that was resistant to cleavage by catS (14), but this has not been completed for catL and catS. Instructions for using PACMANS are provided (*SI Appendix*).

This distraction interaction is a competitive inhibitor interaction, defined as a cathepsin's ability to reversibly bind to an inactive cathepsin and catalyze the inactive enzyme to a degraded form, as described here. There are a number of physiological scenarios where distraction cathepsin could be produced and affect the network interactions. Under natural conditions in cells and tissue, these distraction interactions may serve to protect substrates from degradation. Cathepsin distractions could also be generated when cysteine cathepsins are secreted into more neutral extracellular environments where cathepsins can rapidly inactivate, losing their proteolytic activity, as they would no longer be in the preferred acidic, reducing environment of lysosomes. The catS, however, retains activity at neutral pH (2, 36, 37) and could bind and degrade other inactive cathepsins according to the rates and affinities (*SI Appendix*, Table S1), instead of target substrate.

Under pharmaceutical therapeutic conditions, distraction could occur following binding to an irreversible protease inhibitor, causing accumulation of inhibitor bound protease. This could become a distracting species, susceptible to being bound by other proteases in a catalytically active conformation, but unable to bind or hydrolyze substrate. Translating cathepsin inhibitors from bench to bedside has been fraught with side effects that have canceled human clinical trials (16, 38, 39), with odanacatib

being the most recent example (40). Accurately targeting cathepsins with well-designed inhibitors has been achieved, but side effects that result due to one of two scenarios: 1) inhibited cathepsins become substrates for other cathepsins and distract them from their targets, or 2) inhibited cathepsins lose their ability to hydrolyze another cathepsin. This could allow for other cathepsin levels to be above normal and proteolyze more of the cathepsin's targets than it would have under homeostatic, nonperturbed conditions. Balicatib, odanacatib, and ONO-5334 are three catK inhibitors that showed beneficial effects for treating bone resorption, but off-target effects precluded their movement through the pipeline (41–44). Odanacatib was the most promising catK inhibitor, and was even fast-tracked through phase II and phase III clinical trials, as it reduced vertebral hip and nonvertebral fractures compared to placebo and increased lumbar spine and total hip bone density (45–47). However, a risk of stroke in Phase 3 Long-term Odanacatib Fracture Trial (NCT00529373) (40) ended further studies of odanacatib and its submission to FDA for approval. Interestingly, however, the individuals with arrhythmias were different from those who had strokes, and the strokes were ischemic, not hemorrhagic. Arrhythmias generate thrombi that can cause ischemic strokes, so it is difficult to link the increased arrhythmias with odanacatib as causal mechanisms to the strokes that occurred in the odanacatib treatment group (40). If the amount of free, catalytically active cathepsins was actually lower than anticipated due to binding to inactive or other active

cathepsins in the system, then excess inhibitor could cross-reactively bind to other cathepsins present in the system with lower binding affinities, precipitating side effects. These can be explored and modeled using the Shiny app to test predictions computationally, and identify concentrations of proteases and inhibitors where these reactions would generate the anticipated outcomes.

Absence of catK in a mouse model, however, promoted stable atherosclerotic plaques (48), so the mechanisms underlying catK inhibition and cardiovascular complications are still not clear. Other examples of cathepsin network dysregulation have been shown with cathepsin null mice. The catK deficiency significantly reduced elastinolytic catL and catS expression in smooth muscle cells, but actually caused an increase in catL in the endothelial cells (49), illustrating cell-specific differences after loss of a cathepsin in the network. Also, in catL null mice, there were reduced activities of catK and S in endothelial cells compared to wild-type mice (50). To fit this with our findings here, catL may be serving as a substrate for catK and S, through distraction, which would stabilize catK and S active lifetimes, preventing autodigestion that they would undergo in the absence of any substrate.

In thyroid cell models, Brix and coworkers (51) have shown that cleavage of thyroglobulin in vitro by different combinations of catB, catK, catL, and catS generate different cleavage products than when incubated separately. It was also noted that there was less effective liberation of T4 observed when catK and S were coincubated with thyroxine compared to combinations of catS with catB or L. We posit that the proteases interacting with and cleaving each other may also have been contributing in this system (51). In other work by this group, catL was up-regulated in thyroids of mice null for catK or double null for catB and catK, which the authors suggest could be compensation of catL for catK deficiency (52), but we hypothesize it could also be the case that, in the absence of catK, there was less cannibalism of catL by catK, allowing the steady-state level of catL to be higher than in the wild-type mouse, which is what we simulated in Fig. 4*J*.

Pycnodysostosis is a rare autosomal recessive disease characterized by mutations in the catK gene, resulting in reduced or absent synthesis of catK (29, 30). The in silico scenarios of pycnodysostosis further highlighted the importance of cathepsin cannibalism and distraction in net degradation by the cathepsin proteolytic network. When there was no catK present (Fig. 4*G*) or when the mutant catK could bind substrate, the total substrate degradation was only slightly reduced from when all were present and catalytically active. The catL and catS could focus on hydrolyzing substrate, when catK was occupied and bound to substrate, since our assumption was that only free catK could be bound by another protease. This may not be true under all circumstances, but was appropriate for this model. In the scenario where catK was present but catalytically inactive and unable to bind substrate, catK served as a competitive inhibitor, which was a distraction to the other proteases (catS and catL), reducing substrate degradation based on inactive catK's relative binding affinities vs. substrate (Fig. 4 *H* and *I*). In our previous in vitro studies, we showed that catK reduced the amount of catL in the system when coincubated in the presence of type I collagen (20), which corroborates the data in Fig. 2*I*, where introducing catK reduced the amount of catL protein. This was also supported in Fig. 4 *J* and *M*, indicating that, when there was no catK present, or catK was inactive, as in the pycnodysostosis modeled cases, there was an increased amount of catL in system.

In all three scenarios modeling pycnodysostosis, there was an increase in the amount of active catL (Fig. 4 *J–O*), highlighting the significance of cannibalism and distraction reactions in cathepsin proteolytic network dynamics. These hypothesized increases in active catL due to reduced cannibalism by catK, and, potentially, catS by binding inactive catK, preventing its inactivation. Increasing the steady-state amounts of catL and catS may have consequences for their other substrates, especially if

they are signaling molecules or signaling intermediates that are now at greater susceptibility to hydrolysis, further muddling potential intuition about cellular responses to proteolytic network perturbations. As an example, catL hydrolyzes collagen XVIII to release the fragment endostatin that has vasoactive functions (53). Increased catL due to inhibition or absent catK could cause elevated vasoconstriction, due to increased endostatin generation in that system. The catS also can modulate endostatin's anti-angiogenic activity (54), further motivating integration of these activities into a computational proteolytic network.

Other protease families contain members that hydrolyze each other, but, to our knowledge, these proteolytic events activate a zymogen or inactive form, converting it to the mature, active protease form; we are describing destructive hydrolysis as a consequence of cathepsin cannibalism or autodigestion. Zymogen activation occurs with digestive system enzymes pepsinogen, trypsinogen, and chymotrypsinogen and also for coagulation cascade to active serine proteases that culminate in cleavage of prothrombin to thrombin and fibrin matrix polymerization (55). Caspases are another system of proteases that cleave procaspases to the active caspase forms as a part of the apoptotic cascade, which then go and proteolyze their cellular targets (56). Cysteine cathepsins contribute to each of these functional responses (57, 58), so there also may be interproteolytic family interactions in a more complex proteolytic network. For cysteine cathepsins, mature cathepsins cleave the propeptide from another procathepsin, activating it to the mature form. Interfamilial proteolysis occurs here as well, since it is established that the aspartic protease catD can activate many procathepsins to the mature form. Thus, cathepsins inactivate other cathepsins by their hydrolytic activity, which presents different consequences of the system.
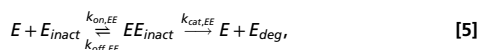
A limitation to these assumptions and application of this model are that dynamics of the proteolytic network are affected by local microenvironmental factors, such as pH, suggesting that the relative contributions of the various processes that contribute to cathepsin loss would also be microenvironment-dependent, requiring some reconfiguring of the parameters. The ECM substrates are also insoluble, complex macromolecules that are not homogeneously mixed; however, as they are hydrolyzed, soluble fragments are released that will diffuse and be susceptible to further degradation in that volume where the proteases are active. Cells can even create compartments around insoluble ECM proteins, locally acidify that space, and release proteases. This is demonstrated for macrophages degrading elastin (59) and is well established for osteoclasts forming lacunae to resorb bone and hydrolyze collagen using catK (60–62). These interactions could also be in play on non-ECM substrates, in the confines of the lysosomes/endosomes with multiple substrates present, and other spaces where multiple proteases are present and active. We are developing a generalized interface that will allow users to choose the number of proteases that compose the proteolytic network being examined and to input their own kinetic parameters, or simply explore the kinetic parameters in a hypothetical proteolytic network.

Methods

Recombinant or Isolated Cathepsin and Fluorogenic Protein Degradation. Recombinant catK, catL, and catS were used in substrate degradation studies. Details of enzyme and substrate purification and characterization are provided in *SI Appendix*. Kinetic studies of substrate degradation monitor fluorescence released when the substrate was cleaved, and incubated with different combinations of recombinant or isolated catK, L, and S to determine time series substrate degradation over 120 min. EnzChek Gelatinase Assay Kit (Thermo Fisher) was performed in a 96-well plate with each well receiving 50 μL of 150 μg/mL DQ-gelatin, 5 pmol of each enzyme, and cathepsin assay buffer (0.1 M sodium phosphate buffer, pH 6.0, 1 mM ethylenediaminetetraacetic acid [EDTA], and 2 mM dithiothreitol [DTT]) used to fill each well to 150 μL. Three coincubation scenarios were examined and compared to the control of substrate only: (1) each cathepsin's gelatinase activity alone, 2) gelatinase activity by cathepsin pairs (i.e., equimolar
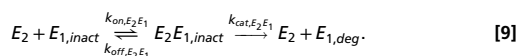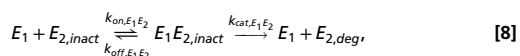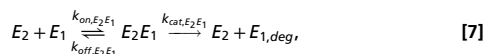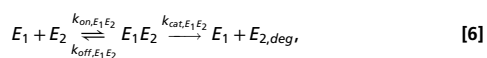
amounts of catK and S, S and L, etc.), and 3) gelatinase activity by all three cathepsins at once. These cases were used to determine kinetic rates in the development of the cathepsin proteolytic computational model to determine substrate degradation attributed to each cathepsin. We have repeated this experiment at least three independent times with different combinations of the proteases, and the trends in the results were reflected across the independent experimental runs. For the model, the data from one comprehensive experiment that included all experimental conditions with the same batch of recombinant or isolated proteases were run with two technical replicates in a 96-well plate. These data were used for fitting and parameter estimation discussed in the study.

Mechanistic Model Development. For each individual cathepsin, mass action kinetics was used to describe the reactions presented here,

$$E + S \underset{k_{off}}{\overset{k_{on}}{\rightleftharpoons}} ES \overset{k_{cat}}{\rightarrow} E + P, \tag{2}$$

$$E \overset{k_{inact}}{\longrightarrow} E_{inact}, \tag{3}$$

$$E + E \underset{k_{off,EE}}{\overset{k_{on,EE}}{\rightleftharpoons}} EE \overset{k_{cat,EE}}{\longrightarrow} E + E_{deg}, \tag{4}$$

$$E + E_{inact} \underset{k_{off,EE}}{\overset{k_{on,EE}}{\rightleftharpoons}} EE_{inact} \overset{k_{cat,EE}}{\longrightarrow} E + E_{deg}, \tag{5}$$

where E represents the enzyme (cathepsin) and S was the substrate (gelatin or elastin). ES was the complex that forms between the enzyme and substrate, which was catalyzed to free enzyme, E, and product formation (degraded substrate), P. Eq. **2** describes the reactions involved in substrate hydrolysis, while Eqs. **3** to **5** describe reactions involved in the loss of active enzyme. There was a rate at which the enzyme was inactivated over time (k_{inact}). Enzyme, E, was able to bind to either another molecule of free enzyme, E, ultimately leading to autodigestion of active enzyme and the formation of degraded enzyme, E_{deg}. Enzyme also formed reversible complexes with E_{inact}, EE_{inact}, which can also lead to the formation of E_{deg}. Sets of differential equations were constructed for each cathepsin (catK, catL, and catS) on gelatin and elastin substrates. The kinetic parameters (k_{on}, k_{off}, k_{cat}, $k_{on,EE}$, $k_{off,EE}$, $k_{cat,EE}$, and k_{inact}) were estimated using the dataset gathered based on fluorogenic substrate assays. The initial conditions for the systems were 33 nM active and 0 nM inactive enzyme, with 1.3 µM substrate if modeling gelatin or 0.7 µM substrate if modeling elastin. Concentrations of product, P, and all intermediate complexes were assumed to initially be 0 nM.

Once kinetics for each individual cathepsin on each substrate were determined, cathepsin cannibalism and distraction interaction terms were introduced, with the addition of an equimolar amount of a different cathepsin. Mass action kinetics describe these interactions as shown by

$$E_1 + E_2 \underset{k_{off,E_1E_2}}{\overset{k_{on,E_1E_2}}{\rightleftharpoons}} E_1E_2 \overset{k_{cat,E_1E_2}}{\longrightarrow} E_1 + E_{2,deg}, \tag{6}$$

$$E_2 + E_1 \underset{k_{off,E_2E_1}}{\overset{k_{on,E_2E_1}}{\rightleftharpoons}} E_2E_1 \overset{k_{cat,E_2E_1}}{\longrightarrow} E_2 + E_{1,deg}, \tag{7}$$

$$E_1 + E_{2,inact} \underset{k_{off,E_1E_2}}{\overset{k_{on,E_1E_2}}{\rightleftharpoons}} E_1E_{2,inact} \overset{k_{cat,E_1E_2}}{\longrightarrow} E_1 + E_{2,deg}, \tag{8}$$

$$E_2 + E_{1,inact} \underset{k_{off,E_2E_1}}{\overset{k_{on,E_2E_1}}{\rightleftharpoons}} E_2E_{1,inact} \overset{k_{cat,E_2E_1}}{\longrightarrow} E_2 + E_{1,deg}. \tag{9}$$

Appropriate terms were included with the differential equations, and the interaction parameters (six parameters, in total, for each pair) were fitted to the paired cathepsin substrate degradation data, while the self-interaction,

inactivation, and enzyme-substrate parameters were fixed to the values found in the initial stage. Similar terms were included in the differential equations for all cathepsins. Once the individual kinetics and paired kinetic parameters were determined, elastin and gelatin substrate degradations for all three cathepsins at once could be predicted a priori.

Parameter Estimation. To guide the parameter estimation to find the optimal parameter set, the cathepsin proteolytic network parameters were fit systematically, compared with experimental data, and the parameters were validated with a priori predictions. Initial parameter bounds were based on reported ranges of K_M and k_{cat} values (63). Furthermore, the on-rate upper bound was set by diffusion limit (63), and the off-rate lower bound was based on biotin−streptavidin affinity, which is the strongest noncovalent biological interaction known (64, 65).

$$10^{-6}s^{-1}pM^{-1} \leq k_{on} \leq 10^{-3}s^{-1}pM^{-1}, \tag{10}$$

$$10^{-5}s^{-1} \leq k_{off} \leq 10^{2}s^{-1}, \tag{11}$$

$$0 \leq k_{cat} \leq 10^{3}s^{-1}. \tag{12}$$

The cathepsin−cathepsin interactions were assumed to be independent of the substrates. Parameters for cathepsin−cathepsin interactions, as well as rates of inactivation, were therefore constrained to agree across substrates, which required fitting the parameters for elastin and gelatin simultaneously. Our framework utilizes a recently developed surrogate-based optimization algorithm (66), aimed at minimizing the number of parameter sets that have to be evaluated. See *SI Appendix* for detailed descriptions of parameter fitting methodology.

After identifying parameters for catK, L, and S individually, the cathepsin cannibalism and distraction terms were fitted for each of the paired combinations of cathepsins. When fitting the cannibalism and distraction terms, the parameters fitted based on the individual cathepsins were fixed to the identified values. The case with three cathepsins allowed for a priori confirmation of these cannibalistic relationships. Additional, in silico scenarios were simulated with the computational model to predict the effects of cathepsin−cathepsin interactions on the cathepsin proteolytic network.

Interactive Online Model Interface. Following the parameterization of the proteolytic network model, we developed an interactive online interface using the R statistical programming language and the R Shiny (31) framework. The developed R Shiny application allows users to manipulate initial cathepsin and substrate concentrations, as well as to introduce cathepsin inhibitors to predict the effects on substrate degradation and cathepsin concentrations. The application utilizes R Shiny slider widgets to allow easy manipulation of model parameters and initial conditions, while the R package deSolve (32) is used to numerically integrate the model equations given the latest model inputs, and R plotly (33) is used to generate interactive plots of model outputs in real time. Interactive plots have been included to visualize concentrations of degraded substrate, active/inactive proteases, protease complexes, and degraded proteases, while also including breakdowns with respect to the contributions of each cathepsin. Additionally, R Markdown (34) is also utilized to generate HTML reports that summarize the model predictions, given the selected model inputs.

Software Availability. All data and the software code are available at Mendeley Data (https://data.mendeley.com/datasets/k2h7y57sd8/1) (21). The interactive, online interface supporting these findings is available at https://plattlab.shinyapps.io/catKLS/ (shown in Fig. 5).

1. N. Fortelny et al., Network analyses reveal pervasive functional regulation between proteases in the human protease web. *PLoS Biol.* **12**, e1001869 (2014).
2. H. A. Chapman, R. J. Riese, G. P. Shi, Emerging roles for cysteine proteases in human biology. *Annu. Rev. Physiol.* **59**, 63–88 (1997).
3. M. E. McGrath, The lysosomal cysteine proteases. *Annu. Rev. Biophys. Biomol. Struct.* **28**, 181–204 (1999).
4. A. H. Aguda et al., Structural basis of collagen fiber degradation by cathepsin K. *Proc. Natl. Acad. Sci. U.S.A.* **111**, 17474–17479 (2014).
5. D. Brömme, Z. Li, M. Barnes, E. Mehler, Human cathepsin V functional expression, tissue distribution, electrostatic surface potential, enzymatic characterization, and chromosomal localization. *Biochemistry* **38**, 2377–2385 (1999).

6. Z. Li et al., Regulation of collagenase activities of human cathepsins by glycosaminoglycans. *J. Biol. Chem.* **279**, 5470–5479 (2004).
7. P. Panwar et al., Effects of cysteine proteases on the structural and mechanical properties of collagen fibers. *J. Biol. Chem.* **288**, 5940–5950 (2013).
8. Y. Yasuda et al., Cathepsin V, a novel and potent elastolytic activity expressed in activated macrophages. *J. Biol. Chem.* **279**, 36761–36770 (2004).
9. M. S. McQueney et al., Autocatalytic activation of human cathepsin K. *J. Biol. Chem.* **272**, 13955–13960 (1997).
10. O. Vasiljeva, M. Dolinar, J. R. Pungercar, V. Turk, B. Turk, Recombinant human procathepsin S is capable of autocatalytic processing at neutral pH in the presence of glycosaminoglycans. *FEBS Lett.* **579**, 1285–1290 (2005).

11. R. Ménard *et al.*, Autocatalytic processing of recombinant human procathepsin L. Contribution of both intermolecular and unimolecular events in the processing of procathepsin L in vitro. *J. Biol. Chem.* **273**, 4478–4484 (1998).

12. Z. T. Barry, M. O. Platt, Cathepsin S cannibalism of cathepsin K as a mechanism to reduce type I collagen degradation. *J. Biol. Chem.* **287**, 27723–27730 (2012).

13. J. Christensen, V. P. Shastri, Matrix-metalloproteinase-9 is cleaved and activated by cathepsin K. *BMC Res. Notes* **8**, 322 (2015).

14. M. C. Ferrall-Fairbanks *et al.*, PACMANS: A bioinformatically informed algorithm to predict, design, and disrupt protease-on-protease hydrolysis. *Protein Sci.* **26**, 880–890 (2017).

15. J. Reiser, B. Adair, T. Reinheckel, Specialized roles for cysteine cathepsins in health and disease. *J. Clin. Invest.* **120**, 3421–3431 (2010).

16. D. Brömme, F. Lecaille, Cathepsin K inhibitors for osteoporosis and potential off-target effects. *Expert Opin. Investig. Drugs* **18**, 585–600 (2009).

17. D. Brömme, P. Panwar, S. Turan, Cathepsin K osteoporosis trials, pycnodysostosis and mouse deficiency models: Commonalities and differences. *Expert Opin. Drug Discov.* **11**, 457–472 (2016).

18. C. Le Gall, E. Bonnelye, P. Clézardin, Cathepsin K inhibitors as treatment of bone metastasis. *Curr. Opin. Support. Palliat. Care* **2**, 218–222 (2008).

19. A. N. Parks *et al.*, Supraspinatus tendon overuse results in degenerative changes to tendon insertion region and adjacent humeral cartilage in a rat model. *J. Orthop. Res.* **35**, 1910–1918 (2016).

20. A. N. Parks, J. Nahata, N. E. Edouard, J. S. Temenoff, M. O. Platt, Sequential, but not concurrent, incubation of cathepsin K and L with type I collagen results in extended proteolysis. *Sci. Rep.* **9**, 5399 (2019).

21. M. Platt, Data for "Reassessing enzyme kinetics: Considering protease-assubstrate interactions in proteolytic networks." Mendeley Data. https://data.mendeley.com/datasets/k2h7y57sd8/1. Deposited 10 January 2020.

22. S. Hoops *et al.*, COPASI–A COmplex PAthway SImulator. *Bioinformatics* **22**, 3067–3074 (2006).

23. C. M. Guldberg, P. Waage, Studier i affiniteten. *Forhandlinger i Videnskabs-Selskabet i Christiania* **1864**, 35–45 (1864).

24. C. M. Guldberg, P. Waage, *Etudes sur les Affinites Chimiques*. (Brogger Christie, 1867).

25. C. M. Guldberg, P. Waage, Uber die chemische Affinitat. *Erdmann's J. fur practische Cehmie* **127**, 69–114 (1879).

26. M. A. Savageau, E. O. Voit, Recasting nonlinear differential equations as S-systems: A canonical nonlinear form. *Math. Biosci.* **87**, 83–115 (1987).

27. D. Brömme, K. Okamoto, B. B. Wang, S. Biroc, Human cathepsin O2, a matrix protein-degrading cysteine protease expressed in osteoclasts. Functional expression of human cathepsin O2 in *Spodoptera frugiperda* and characterization of the enzyme. *J. Biol. Chem.* **271**, 2126–2132 (1996).

28. A. Arman *et al.*, Cathepsin K analysis in a pycnodysostosis cohort: Demographic, genotypic and phenotypic features. *Orphanet J. Rare Dis.* **9**, 60 (2014).

29. G. Motyckova, D. E. Fisher, Pycnodysostosis: Role and regulation of cathepsin K in osteoclast function and human disease. *Curr. Mol. Med.* **2**, 407–421 (2002).

30. B. D. Gelb, G. P. Shi, H. A. Chapman, R. J. Desnick, Pycnodysostosis, a lysosomal disease caused by cathepsin K deficiency. *Science* **273**, 1236–1238 (1996).

31. W. Chang, J. Cheng, J. J. Allaire, Y. Xie, J. McPherson, R shiny: Web Application Framework for R. Version 1.3.2. https://cran.r-project.org/web/packages/shiny/index.html. Accessed 12 May 2019.

32. K. Soetaert, T. Petzoldt, R. W. Setzer, Solving differential equations in R: Package deSolve. *J. Stat. Softw.* **33**, 1–25 (2010).

33. C. Sievert, R plotly. Version 4.9.0. https://cran.r-project.org/web/packages/plotly/index.html. Accessed 12 May 2019.

34. J. J. Allaire, J. Horner, Y. Xie, V. Marti, N. Porte, R markdown: 'Markdown' Rendering for R. Version 0.9. https://cran.r-project.org/web/packages/markdown/index.html. Accessed 12 May 2019.

35. K. Brix, A. Dunkhorst, K. Mayer, S. Jordans, Cysteine cathepsins: Cellular roadmap to different functions. *Biochimie* **90**, 194–207 (2008).

36. D. Brömme *et al.*, Functional expression of human cathepsin S in *Saccharomyces cerevisiae*. Purification and characterization of the recombinant enzyme. *J. Biol. Chem.* **268**, 4832–4838 (1993).

37. C. L. Wilder, K. Y. Park, P. M. Keegan, M. O. Platt, Manipulating substrate and pH in zymography protocols selectively distinguishes cathepsins K, L, S, and V activity in cells and tissues. *Arch. Biochem. Biophys.* **516**, 52–57 (2011).

38. A. Lee-Dutra, D. K. Wiener, S. Sun, Cathepsin S inhibitors: 2004-2010. *Expert Opin. Ther. Pat.* **21**, 311–337 (2011).

39. Y. Y. Li, J. Fang, G. Z. Ao, Cathepsin B and L inhibitors: A patent review (2010–present). *Expert Opin. Ther. Pat.* **27**, 643–656 (2017).

40. A. Mullard, Merck &Co. drops osteoporosis drug odanacatib. *Nat. Rev. Drug Discov.* **15**, 669 (2016).

41. P. Papanastasiou, C. Ortmann, M. Olson, A. Vigneron, U. Trechsel, Effect of three month treatment with the cathepsin-k inhibitor, balicatib, on biochemical markers of bone turnover in postmenopausal women: Evidence for uncoupling of bone resorption and bone formation. *J. Bone Miner. Res.* **21**, S59 (2006).

42. S. Adami *et al.*, Effect of one year treatment with the cathepsin-K inhibitor, balicatib, on bone mineral density (BMD) in postmenopausal women with osteopenia/osteoporosis. *J. Bone Miner. Res.* **21**, S24 (2006).

43. M. Tanaka, Y. Hashimoto, C. Hasegawa, S. Deacon, R. Eastell, Antiresorptive effect of a cathepsin K inhibitor ONO-5334 and its relationship to BMD increase in a phase II trial for postmenopausal osteoporosis. *BMC Musculoskelet. Disord.* **18**, 267 (2017).

44. R. Eastell *et al.*, Effect of the cathepsin K inhibitor ONO-5334 on biochemical markers of bone turnover in the treatment of postmennopausal osteopenia or osteoporosis: 2-year results from the OCEAN study. *J. Bone Miner. Res.* **29**, 458–466 (2014).

45. M. R. McClung *et al.*, Odanacatib anti-fracture efficacy and safety in postmenopausal women with osteoporosis: Results from the phase III long-term odanacatib fracture trial. *Osteoporos. Int.* **25**, 573–575 (2014).

46. M. McClung *et al.*, Ocanacatib antifracture efficacy and saftey in postmenopausal women with osteoporosis: Results from the phase III long-term adonacatib fracture trial (LOFT). *Osteoporos. Int.* **26**, S35–S36 (2015).

47. R. Rizzoli *et al.*, Continuous treatment with odanacatib for up to 8 years in postmenopausal women with low bone mineral density: A phase 2 study. *Osteoporos. Int.* **27**, 2099–2107 (2016).

48. E. Lutgens *et al.*, Disruption of the cathepsin K gene reduces atherosclerosis progression and induces plaque fibrosis but accelerates macrophage foam cell formation. *Circulation* **113**, 98–107 (2006).

49. J. Sun *et al.*, Cathepsin K deficiency reduces elastase perfusion-induced abdominal aortic aneurysms in mice. *Arterioscler. Thromb. Vasc. Biol.* **32**, 15–23 (2012).

50. J. Sun *et al.*, Cathepsin L activity is essential to elastase perfusion-induced abdominal aortic aneurysms in mice. *Arterioscler. Thromb. Vasc. Biol.* **31**, 2500–2508 (2011).

51. S. Jordans *et al.*, Monitoring compartment-specific substrate cleavage by cathepsins B, K, L, and S at physiological pH and redox conditions. *BMC Biochem.* **10**, 23 (2009).

52. B. Friedrichs *et al.*, Thyroid functions of mouse cathepsins B, K, and L. *J. Clin. Invest.* **111**, 1733–1745 (2003).

53. U. Felbor *et al.*, Secreted cathepsin L generates endostatin from collagen XVIII. *EMBO J.* **19**, 1187–1194 (2000).

54. F. Veillard *et al.*, Cysteine cathepsins S and L modulate anti-angiogenic activities of human endostatin. *J. Biol. Chem.* **286**, 37158–37167.

55. R. F. Doolittle, Clotting of mammalian fibrinogens by papain: A re-examination. *Biochemistry* **53**, 6687–6694 (2014).

56. C. E. Chwieralski, T. Welte, F. Bühling, Cathepsin-regulated apoptosis. *Apoptosis* **11**, 143–149 (2006).

57. S. A. Douglas, S. E. Lamothe, T. S. Singleton, R. D. Averett, M. O. Platt, Human cathepsins K, L, and S: Related proteases, but unique fibrinolytic activity. *Biochim. Biophys. Acta Gen. Subj.* **1862**, 1925–1932 (2018).

58. U. Repnik, V. Stoka, V. Turk, B. Turk, Lysosomes and lysosomal cathepsins in cell death. *Biochim. Biophys. Acta* **1824**, 22–33 (2012).

59. A. Punturieri *et al.*, Regulation of elastolytic cysteine proteinase activity in normal and cathepsin K-deficient human macrophages. *J. Exp. Med.* **192**, 789–799 (2000).

60. S. L. Teitelbaum, Bone resorption by osteoclasts. *Science* **289**, 1504–1508 (2000).

61. H. K. Väänänen, M. Horton, The osteoclast clear zone is a specialized cell-extracellular matrix adhesion structure. *J. Cell Sci.* **108**, 2729–2732 (1995).

62. H. C. Blair, A. J. Kahn, E. C. Crouch, J. J. Jeffrey, S. L. Teitelbaum, Isolated osteoclasts resorb the organic and inorganic components of bone. *J. Cell Biol.* **102**, 1164–1172 (1986).

63. R. Milo, R. Phillips, *Cell Biology by the Numbers* (Garland Science, ed. 1, 2015).

64. N. M. Green, Avidin. *Adv. Protein Chem.* **29**, 85–133 (1975).

65. A. Holmberg *et al.*, The biotin-streptavidin interaction can be reversibly broken using water at elevated temperatures. *Electrophoresis* **26**, 501–510 (2005).

66. C. A. Kieslich, F. Boukouvala, C. A. Floudas, Optimization of black-box problems using Smolyak grids and polynomial approximations. *J. Glob. Optim.* **71**, 845–869 (2018).